Stochastic 3D modeling of the nanoporous binder-additive phase in battery electrodes

Matthias Neumann
Joint work with Phillip Gräfensteiner and Volker Schmidt
September 24, 2024

TU Graz
SCIENCE
PASSION
TECHNOLOGY

Functional materials: Process-structure-property

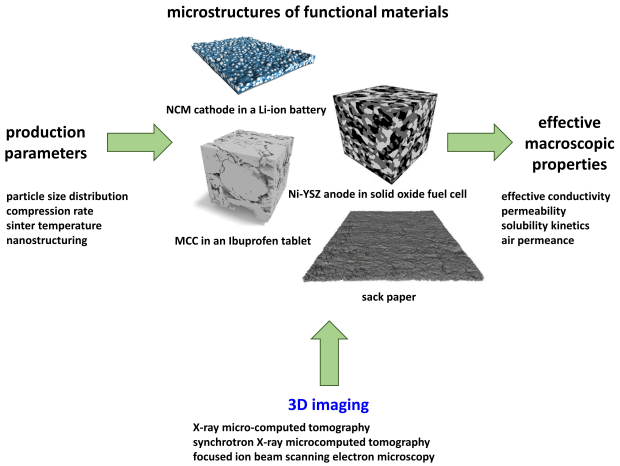

Direct morphological approach

microstructures of functional materials

statistical image analysis

tomographic image data of Ni-YSZ anode in solid oxide fuel cell

Direct morphological approach

microstructures of functional materials

tomographic image data of Ni-YSZ anode in solid oxide fuel cell

statistical image analysis

well-defined microstructure characteristics

Direct morphological approach

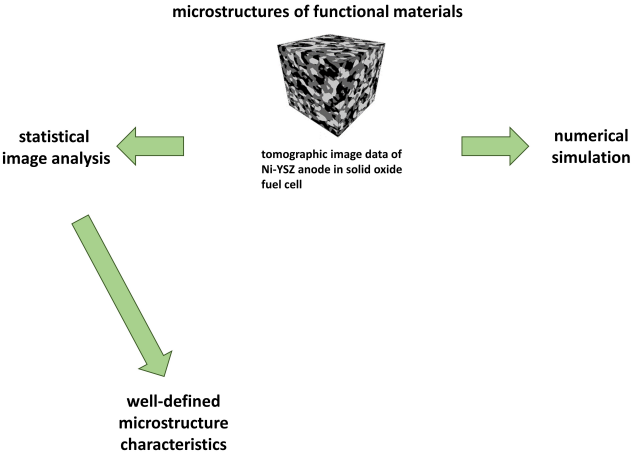

Direct morphological approach

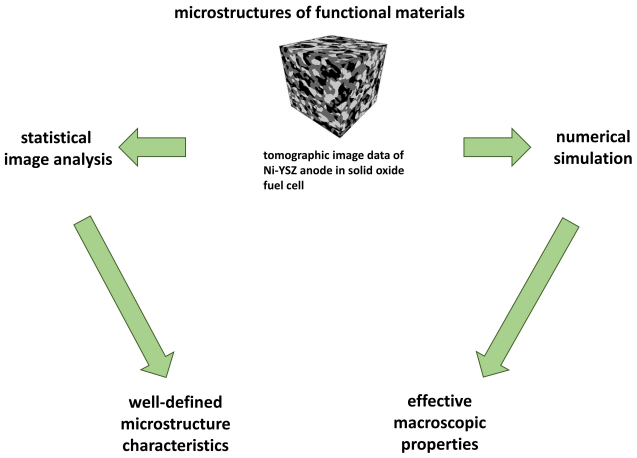

Direct morphological approach

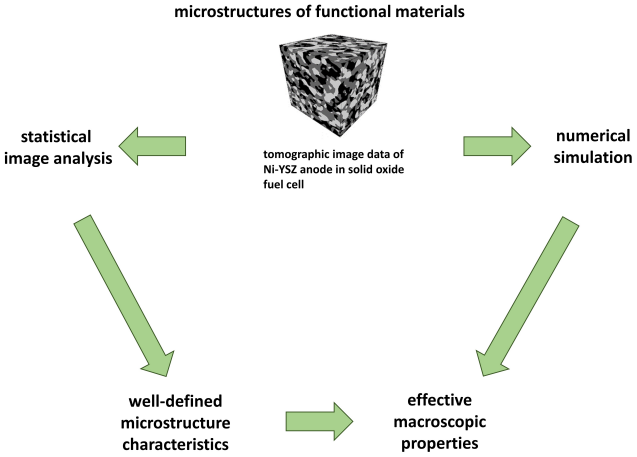

Virtual materials testing

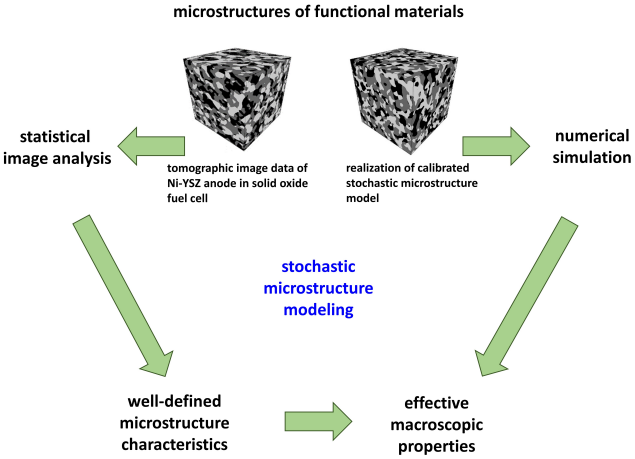

Virtual materials testing

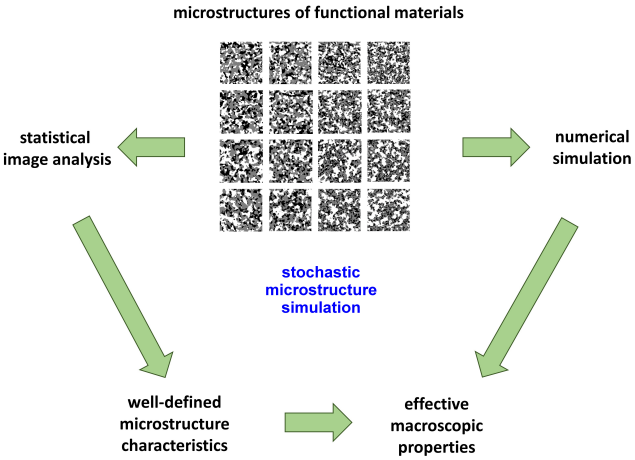

Tomographic image data

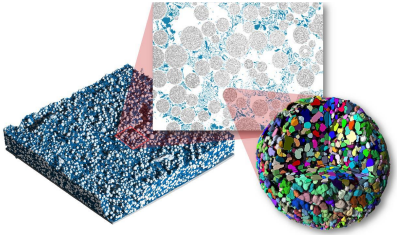

Hierarchically structured NMC-cathode

Wagner, Bohn, Geßwein, Neumann, Osenberg, Hilger, Manke, Schmidt, Binder. *ACS Appl. Energy Mater.* 3 (2020), 12565–12574.

Osenberg, Hilger, Neumann, Wagner, Bohn, Binder, Schmidt, Banhart, Manke. *J. Power Sources* 570 (2023), 233030.

Neumann, Wetterauer, Osenberg, Hilger, Gräfensteiner, Wagner, Bohn, Binder, Manke, Carraro, Schmidt. *Int. J. Solids Struct.* 280 (2023), 112394.

Neumann, Philipp, Neusser, Häringer, Binder, Kranz. *Batter. Supercaps* 7 (2024), 7:e202300409.

Carbon binder domain surrounding active material

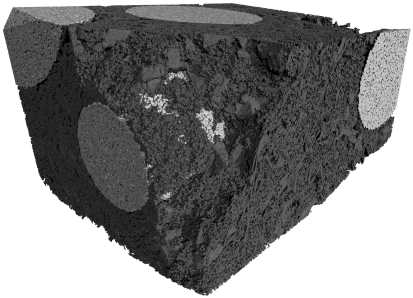

- Active material particles are embedded in a *nanoporous carbon binder domain*
- The nanostructure is resolved by *FIB-SEM tomography*
- Voxel size: 20 nm

Cadiou, Douillard, Willot, Badot, Lestriez, Maire. *J. Electrochem. Soc.* 167 (2020), 140504.

Kroll, Karstens, Cronau, Höltzel, Schlabach, Nobel, Redenbach, Roling, Tallarek. *Batter. Supercaps* 4 (2021), 1363–1373.

Segmentation of graphite particles

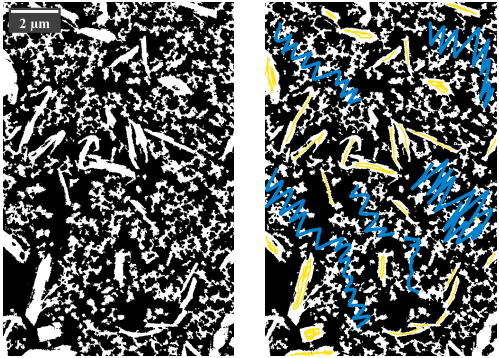

- Large oblate-shaped objects represent *graphite* particles
- The finer structure represents *carbon black*
- Image segmentation performed by *Ilastik* using hand-labeled slices

Berg, Kutra, Kroeger, Straehle, Kausler, Haubold, Schiegg, Ales, Beier, Rudy, Eren, Cervantes, Xu, Beuttenmueller, Wolny, Zhang, Koethe, Hamprecht, Kreshuk. (2019). *Nature Methods*, 16:1226–1232.

Segmentation of graphite particles

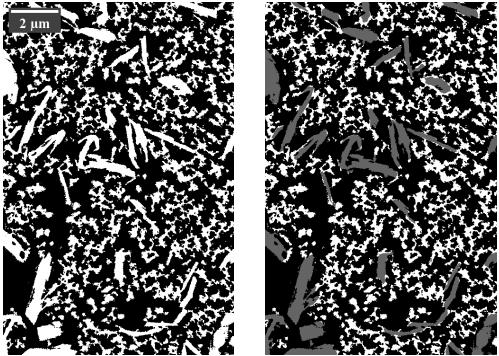

- Large oblate-shaped objects represent *graphite* particles
- The finer structure represents *carbon black*
- Image segmentation performed by *Ilastik* using hand-labeled slices

Modeling idea

Three-step approach

1. *Graphite particles* are modeled by a Boolean model, where the grains are given by oblate spheroids

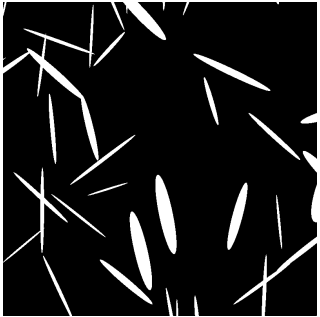

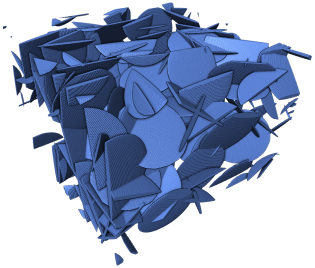

Modeling idea

Three-step approach

2. The union of *PVDF binder and carbon* is modeled by an excursion set of Gaussian random fields

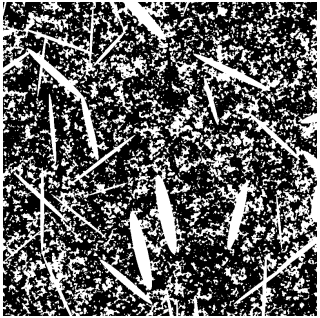

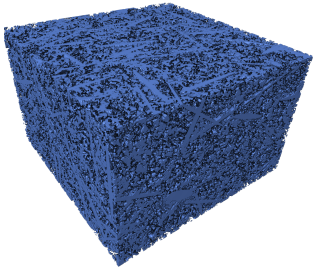

Modeling idea

Three-step approach

3. *Large pore regions* are modeled by a second Boolean model with spherical grains

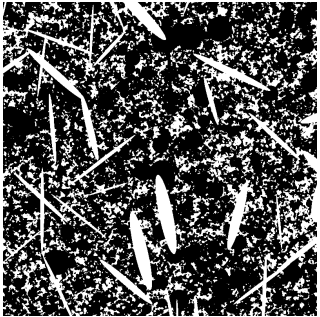

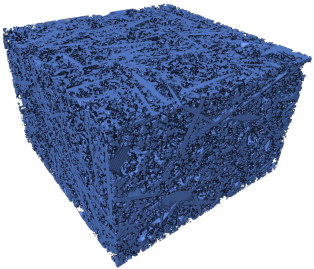

Step 1: Graphite particles–model definition

Boolean model with oblate spheroids as grains

- Let $X_1, X_2, \ldots$ be a homogeneous Poisson point process in $\mathbb{R}^3$ with intensity $\lambda_X > 0$. Let E be a random oblate spheroid centered at the origin with random equatorial radius A and pole-to-centre distance $C \leq A$. Moreover, let the direction of the shorter semi-axis be uniformly distributed on the unit sphere.
- $A = \max\{W_1, W_2\}$ and $C = \min\{W_1, W_2\}$, where W_1, W_2 are independent with $W_1 \sim \Gamma(\alpha_1, \alpha_3)$, $W_2 \sim \Gamma(\alpha_2, \alpha_3)$ for model parameters $\alpha_1, \alpha_2, \alpha_3 > 0$.
- For i.i.d copies $E_1, E_2, \ldots$ of E, define the union of graphite particles by $\Xi_1 = \cup_{i=1}^{\infty} X_i + E_i$

Step 1: Graphite particles–model definition

Boolean model with oblate spheroids as grains

- Let $X_1, X_2, \ldots$ be a homogeneous Poisson point process in $\mathbb{R}^3$ with intensity $\lambda_X > 0$. Let E be a random oblate spheroid centered at the origin with random equatorial radius A and pole-to-centre distance $C \leq A$. Moreover, let the direction of the shorter semi-axis be uniformly distributed on the unit sphere.
- $A = \max\{W_1, W_2\}$ and $C = \min\{W_1, W_2\}$, where W_1, W_2 are independent with $W_1 \sim \Gamma(\alpha_1, \alpha_3)$, $W_2 \sim \Gamma(\alpha_2, \alpha_3)$ for model parameters $\alpha_1, \alpha_2, \alpha_3 > 0$.
- For i.i.d copies $E_1, E_2, \ldots$ of E, define the union of graphite particles by $\Xi_1 = \cup_{i=1}^{\infty} X_i + E_i$

Step 1: Graphite particles–model definition

Boolean model with oblate spheroids as grains

- Let $X_1, X_2, \ldots$ be a homogeneous Poisson point process in $\mathbb{R}^3$ with intensity $\lambda_X > 0$. Let E be a random oblate spheroid centered at the origin with random equatorial radius A and pole-to-centre distance $C \leq A$. Moreover, let the direction of the shorter semi-axis be uniformly distributed on the unit sphere.
- $A = \max\{W_1, W_2\}$ and $C = \min\{W_1, W_2\}$, where W_1, W_2 are independent with $W_1 \sim \Gamma(\alpha_1, \alpha_3)$, $W_2 \sim \Gamma(\alpha_2, \alpha_3)$ for model parameters $\alpha_1, \alpha_2, \alpha_3 > 0$.
- For i.i.d copies $E_1, E_2, \ldots$ of E, define the union of graphite particles by $\Xi_1 = \cup_{i=1}^{\infty} X_i + E_i$

Step 1: Graphite particles–model fitting

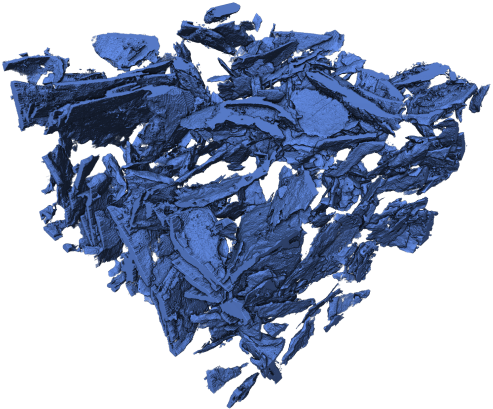

Graphite particles extracted from image data

Step 1: Graphite particles–model fitting

Fit parameters $\lambda_X, \alpha_1, \alpha_2, \alpha_3$

- Fitting is based on volume fraction, surface area per unit volume, specific integral of mean curvature and the specific Euler number, which are estimated from image data.
- The above mentioned descriptors can be expressed as expectations of functions that depend on A, C, and λ_X (Mile's formulae).
- Numerical fitting by the Nelder-Mead algorithm.

Step 1: Graphite particles–model fitting

Fit parameters $\lambda_X, \alpha_1, \alpha_2, \alpha_3$

- Fitting is based on volume fraction, surface area per unit volume, specific integral of mean curvature and the specific Euler number, which are estimated from image data.
- The above mentioned descriptors can be expressed as expectations of functions that depend on A, C, and λ_X (Mile's formulae).
- Numerical fitting by the Nelder-Mead algorithm.

Step 2: PVdF binder and carbon–model definition

Excursion set of a Gaussian random field

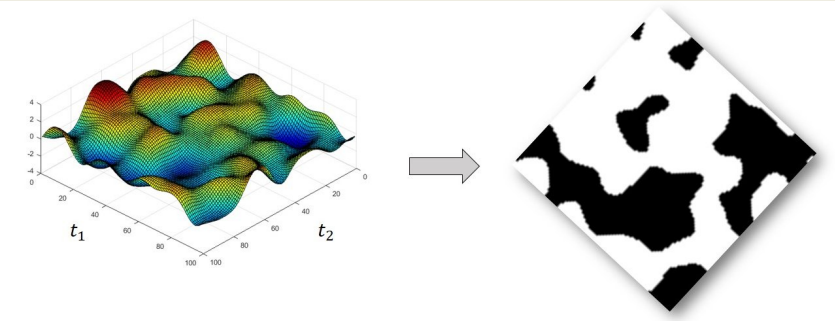

Step 2: PVdF binder and carbon–model definition

Excursion set of a Gaussian random field

- Let $Z = \{Z(t) : t \in \mathbb{R}^3\}$ be a stationary and isotropic Gaussian random field with covariance function ρ such that $\mathbb{E}[Z(t)] = 0$ and $\mathrm{Var}[Z(t)] = 1$ for each $t \in \mathbb{R}^3$.
- Define the union of PVdF binder and carbon by $\Xi_2 \setminus \Xi_1$, where $\Xi_2 = \{t \in \mathbb{R}^3 : Z(t) \geq \mu\}$

Step 2: PVdF binder and carbon–model definition

Excursion set of a Gaussian random field

- Let $Z = \{Z(t) : t \in \mathbb{R}^3\}$ be a stationary and isotropic Gaussian random field with covariance function ρ such that $\mathbb{E}[Z(t)] = 0$ and $\mathrm{Var}[Z(t)] = 1$ for each $t \in \mathbb{R}^3$.
- Define the union of PVdF binder and carbon by $\Xi_2 \setminus \Xi_1$, where $\Xi_2 = \{t \in \mathbb{R}^3 : Z(t) \geq \mu\}$

Step 2: PVdF binder and carbon–model fitting

Fitting the level μ and the covariance function ρ

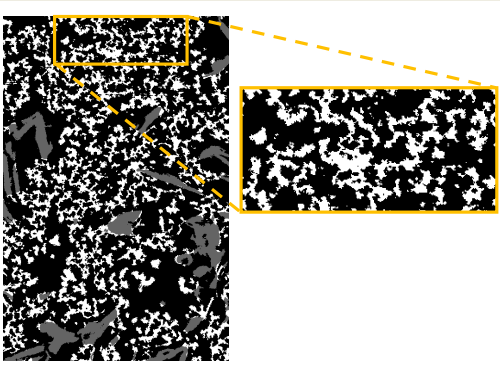

Manually selected homogeneous cutout of PVdF binder and carbon

Step 2: PVdF binder and carbon–model fitting

Fitting the level μ and the covariance function ρ

- The level μ is fitted such that the expected volume fraction in the model coincides with the volume fraction estimated from image data.
- For fitting ρ, we use

$$C(h) := P(s \in \Xi_2, t \in \Xi_2) = V_2^2 + \int_0^{\rho(h)} \frac{e^{\frac{-\mu^2}{1+t}}}{\sqrt{1-t^2}} \, \mathrm{d}t,$$

for each $h = |s - t|$, where V_2 is the volume fraction of Ξ_2.

Step 2: PVdF binder and carbon–model fitting

Fitting the level μ and the covariance function ρ

- The level μ is fitted such that the expected volume fraction in the model coincides with the volume fraction estimated from image data.
- For fitting ρ, we use

$$C(h) := P(s \in \Xi_2, t \in \Xi_2) = V_2^2 + \int_0^{\rho(h)} \frac{e^{\frac{-\mu^2}{1+t}}}{\sqrt{1-t^2}} \, \mathrm{d}t,$$

for each $h = |s - t|$, where V_2 is the volume fraction of Ξ_2.

Step 2: PVdF binder and carbon–model fitting

Fit of ρ

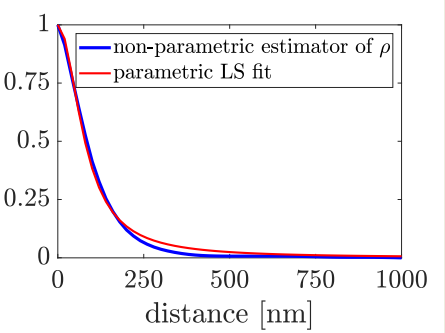

Consider the parametric family of covariance functions

$$\rho(h) = \frac{1}{1 + (\eta h)^2}$$

Step 3: Large pore regions–model definition

Boolean model with spherical grains

- Let $Y_1, Y_2, \ldots$ be a homogeneous Poisson point process in $\mathbb{R}^3$ with intensity $\lambda_Y > 0$. Let $R_1, R_2, \ldots$ be i.i.d random variables with $R_1 \sim \mathrm{Exp}(\theta)$ for some $\theta > 0$.
- Define the union of large pore regions by $\Xi_3 = \cup_{i=1}^{\infty} Y_i + b(o, R_i)$, where $b(o, r)$ is the open ball centered at the origin with radius $r > 0$.
- Model for the binder-additive phase (including graphite particles):

$$\Xi = \Xi_1 \cup (\Xi_2 \setminus \Xi_3).$$

Step 3: Large pore regions–model definition

Boolean model with spherical grains

- Let $Y_1, Y_2, \ldots$ be a homogeneous Poisson point process in $\mathbb{R}^3$ with intensity $\lambda_Y > 0$. Let $R_1, R_2, \ldots$ be i.i.d random variables with $R_1 \sim \mathrm{Exp}(\theta)$ for some $\theta > 0$.
- Define the union of large pore regions by $\Xi_3 = \cup_{i=1}^{\infty} Y_i + b(o, R_i)$, where $b(o, r)$ is the open ball centered at the origin with radius $r > 0$.
- Model for the binder-additive phase (including graphite particles):

$$\Xi = \Xi_1 \cup (\Xi_2 \setminus \Xi_3).$$

Step 3: Large pore regions–model definition

Boolean model with spherical grains

- Let $Y_1, Y_2, \ldots$ be a homogeneous Poisson point process in $\mathbb{R}^3$ with intensity $\lambda_Y > 0$. Let $R_1, R_2, \ldots$ be i.i.d random variables with $R_1 \sim \mathrm{Exp}(\theta)$ for some $\theta > 0$.
- Define the union of large pore regions by $\Xi_3 = \cup_{i=1}^{\infty} Y_i + b(o, R_i)$, where $b(o, r)$ is the open ball centered at the origin with radius $r > 0$.
- Model for the binder-additive phase (including graphite particles):

$$\Xi = \Xi_1 \cup (\Xi_2 \setminus \Xi_3).$$

Step 3: Large pore regions–model fitting

Fitting λ_Y and θ

- For fixed θ, we determine λ_Y such that the expected volume fraction of the model coincides with the value estimated from image data.
- Note that $V = P(o \in \Xi) = P\left(o \in \Xi_1 \cup \left(\Xi_2 \cap \Xi_3^c\right)\right) = V_1 + V_2(1 - V_1)(1 - V_3)$ and

$$V_3 = 1 - \exp\left(\lambda_Y \frac{8\pi}{\theta^3}\right).$$

Step 3: Large pore regions–model fitting

Fitting λ_Y and θ

- Based on simulated model realizations, the parameter θ is determined in order to minimize the L_1-distance to the continuous pore size distribution estimated from image data.
- The continuous pore size distribution is defined as

$$\mathrm{CPSD}(r) = \frac{\mathbb{E}\left[\nu_3\Big(\big(\Xi^c \ominus B(o,r)\big) \oplus B(o,r)\Big)\right]}{\mathbb{E}\big(\nu_3(\Xi^c)\big)},$$

where $B(o,r)$ denotes the closed ball centered at the origin with radius $r > 0$.

Step 3: Large pore regions–model fitting

Fitting λ_Y and θ

- Based on simulated model realizations, the parameter θ is determined in order to minimize the L_1-distance to the continuous pore size distribution estimated from image data.
- The continuous pore size distribution is defined as

$$\mathrm{CPSD}(r) = \frac{\mathbb{E}\left[\nu_3\Big(\big(\Xi^c \ominus B(o,r)\big) \oplus B(o,r)\Big)\right]}{\mathbb{E}\big(\nu_3(\Xi^c)\big)},$$

where $B(o,r)$ denotes the closed ball centered at the origin with radius $r > 0$.

Step 3: Large pore regions–model fitting

Fitting λ_Y and θ

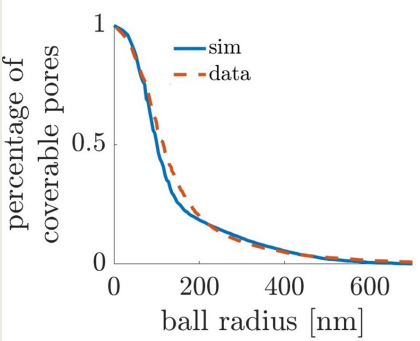

Model validation

Visual comparison

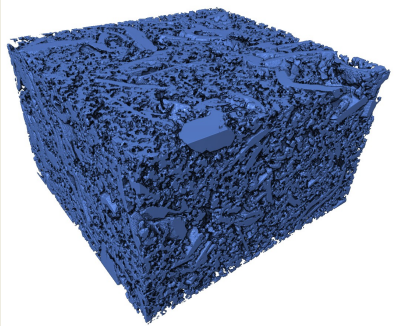

Data

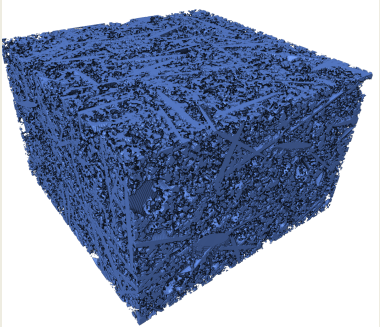

Model realization

Model validation

Comparing morphological descriptors of measured and simulated nanostructures

- mean geodesic tortuosity τ quantifying the length of shortest pathways
- constrictivity β measuring the degree of bottleneck effects
- Two-point coverage probability function C and specific surface area S

Peyrerga, Jeulin (2013). *Image Anal. Stereol.*, 32:27–43.

Neumann, Hirsch, Staněk, Beneš, Schmidt (2019). *Scand. J. Stat.*, 46:848–884.

Model validation

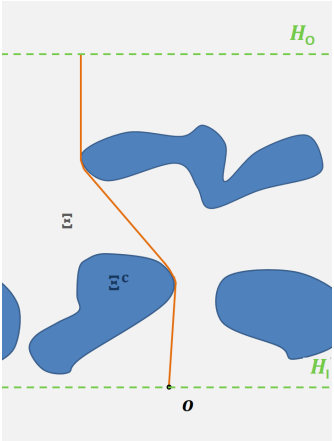

Mean geodesic tortuosity

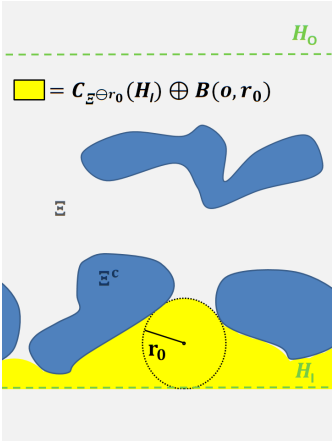

Constrictivity

Model validation

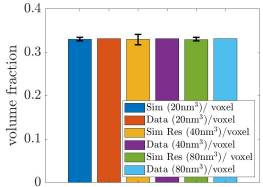

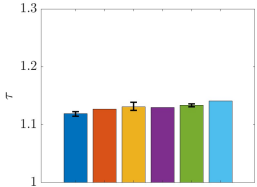

solid phase

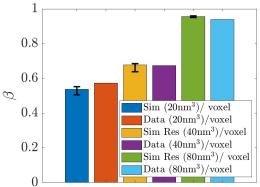

solid phase

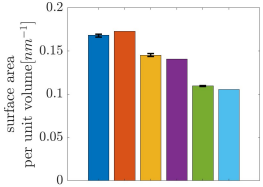

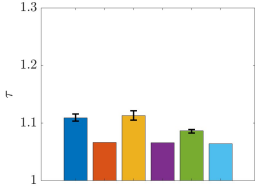

pore phase

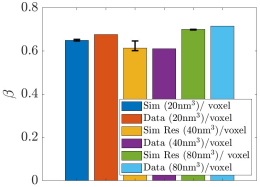

pore phase

Model validation

Two-point coverage functions

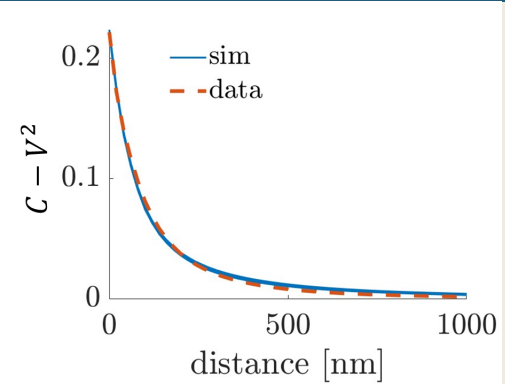

$$C(h) = P(s \in \Xi, t \in \Xi),$$
$$|s - t| = h$$

Effective properties

M-factor

The *M*-factor is defined by

$$M = \sigma_{\mathrm{eff}}/\sigma_0,$$

where σ_{eff} is the *effective* and σ_0 is the *intrinsic conductivity (diffusivity)*.

- Here: *electric conduction* in the solid phase and *diffusion of ions* in the pore space.
- *M*-factor is numerically simulated.

Cooper, Bertei, Shearing, Kilner, Brandon. *SoftwareX* 5 (2016), 203–210.

Effective properties

M-factor

The *M*-factor is defined by

$$M = \sigma_{\mathrm{eff}}/\sigma_0,$$

where σ_{eff} is the *effective* and σ_0 is the *intrinsic conductivity (diffusivity)*.

- Here: *electric conduction* in the solid phase and *diffusion of ions* in the pore space.
- *M*-factor is numerically simulated.

Cooper, Bertei, Shearing, Kilner, Brandon. *SoftwareX* 5 (2016), 203–210.

Effective properties

M-factor

The *M*-factor is defined by

$$M = \sigma_{\mathrm{eff}}/\sigma_0,$$

where σ_{eff} is the *effective* and σ_0 is the *intrinsic conductivity (diffusivity)*.

- Here: *electric conduction* in the solid phase and *diffusion of ions* in the pore space.
- *M*-factor is numerically simulated.

Cooper, Bertei, Shearing, Kilner, Brandon. *SoftwareX* 5 (2016), 203–210.

The role of graphite particles

Simulation study

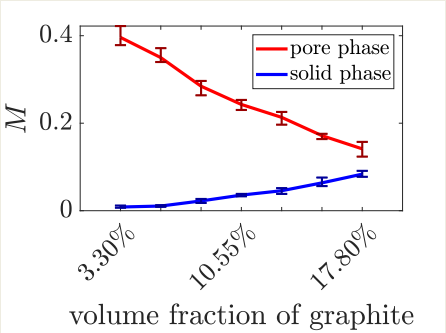

- The volume fraction of graphite particles is varied by varying λ_X.
- All other model parameters remain unchanged.

Conclusions

- A stochastic 3D model has been developed for the carbon binder domain in lithium-ion battery electrodes.
- Boolean models have been combined with excursion sets of Gaussian random fields.
- Model fitting is performed based on segmented 3D image data.
- The validated model is used to study the influence of the amount of graphite particles on effective properties.

Gräfensteiner, Osenberg, Hilger, Bohn, Binder, Manke, Schmidt, Neumann, *arXiv:2409.11080*.

Conclusions

- A stochastic 3D model has been developed for the carbon binder domain in lithium-ion battery electrodes.
- Boolean models have been combined with excursion sets of Gaussian random fields.
- Model fitting is performed based on segmented 3D image data.
- The validated model is used to study the influence of the amount of graphite particles on effective properties.

Gräfensteiner, Osenberg, Hilger, Bohn, Binder, Manke, Schmidt, Neumann, *arXiv:2409.11080*.

Conclusions

- A stochastic 3D model has been developed for the carbon binder domain in lithium-ion battery electrodes.
- Boolean models have been combined with excursion sets of Gaussian random fields.
- Model fitting is performed based on segmented 3D image data.
- The validated model is used to study the influence of the amount of graphite particles on effective properties.

Gräfensteiner, Osenberg, Hilger, Bohn, Binder, Manke, Schmidt, Neumann, *arXiv:2409.11080*.

Conclusions

- A stochastic 3D model has been developed for the carbon binder domain in lithium-ion battery electrodes.
- Boolean models have been combined with excursion sets of Gaussian random fields.
- Model fitting is performed based on segmented 3D image data.
- The validated model is used to study the influence of the amount of graphite particles on effective properties.

Gräfensteiner, Osenberg, Hilger, Bohn, Binder, Manke, Schmidt, Neumann, *arXiv:2409.11080.*